

# Intra-DP: A High Performance Distributed Inference System on Robotic IoT

Anonymous Author(s)

Submission Id: 445\*

## Abstract

The rapid advancements in machine learning (ML) techniques have led to significant achievements in various robotic tasks, where deploying these ML approaches on real-world robots requires fast and energy-efficient inference of their deep neural network (DNN) models. Distributed inference, which involves inference across multiple powerful GPU devices, has emerged as a promising optimization to improve inference performance in modern data centers. However, when deployed over Internet of Things of these real-world robots (robotic IoT), all existing parallel methods (data parallelism, tensor parallelism, pipeline parallelism) fail to simultaneously meet the robots' latency and energy requirements and raise significant challenges due to the failure of data parallelism, the unacceptable communication overhead of tensor parallelism, and the significant transmission bottlenecks in pipeline parallelism due to the limited bandwidth of robotic IoT.

We present Intra-DP, the first high-performance distributed inference system optimized for model inference on robotic IoT. Intra-DP introduces a fine-grained approach to transmission and computation by confining them to each local operator of DNN layers (i.e., operators that can be computed independently without the complete input, such as the convolution kernel in the convolution layer). By adaptively scheduling the computation and transmission of each local operator based on various hardware conditions and network bandwidth, Intra-DP enables different parts of different layers to be computed and transmitted concurrently, and overlap the computation and transmission phases within the same inference task to achieve fast and energy-efficient distributed inference on robotic IoT. The evaluation shows that, Intra-DP reduces inference time by 20% and energy consumption by 10% compared with the state-of-the-art baselines.

**Keywords:** Distributed inference, Robotic IoT, Distributed system and network

## 1 Introduction

The rapid progress in machine learning (ML) techniques has led to remarkable achievements in various fundamental robotic tasks, such as object detection [18, 28, 30], robotic control [22, 44, 54], and environmental perception [4, 23, 49]. However, deploying these ML applications on real-world robots requires fast and energy-efficient inference of their deep neural network (DNN) models, given the need for swift

environmental responses and the limited battery capacity of robots. Placing the entire model on robots not only requires additional computing accelerators on robots (e.g., GPU [34], FPGA [35], SoC [15]), but also introduce additional energy consumption (e.g., 162% more for [30] in our experiments) due to the computationally intensive nature of DNN models, while placing the entire model in the cloud brings an extended response delay.

Distributed inference, which involves inference across multiple GPU devices, has emerged as a promising approach to meet the latency requirements of robotic applications and extend the battery lifetime of robots. This paradigm has been widely adopted in data centers [17, 50, 55], where numerous GPUs are utilized to speed large model inference, such as in the case of ChatGPT [48]. Adopting distributed inference across robots and other powerful GPU devices through the Internet of Things for these robots (robotic IoT) not only accelerates the inference process by leveraging the high computing capabilities of powerful GPUs but also alleviates the local computational burden, thereby reducing energy consumption, making it an ideal solution for robotic applications.

However, all existing parallel methods for distributed inference in the data center are ill-suited for robotic IoT. In data centers, there are mainly three kinds of parallel methods: Data parallelism (DP) replicates the model across devices, and lets each replica handle one mini-batch (i.e., a subset that slices out of an input data set); Tensor parallelism (TP) splits a single DNN layer over devices; Pipeline parallelism (PP) places different layers of a DNN model over devices (layer partitioning) and pipelines the inference to reduce devices' idling time (pipeline execution).

For DP, the small batch sizes inherent to robotic IoT applications (typically 1) hinder the mini-batch computation, rendering DP inapplicable for robotic IoT. In the data center, DP is feasible due to the large batch sizes employed (e.g., 16 images), allowing for the division of inputs into mini-batches that still contain several complete inputs (e.g., 2 images). However, in robotic IoT, real-time performance is crucial, necessitating immediate inference upon receiving inputs, which typically have smaller batch sizes (e.g., 1 image). Further splitting these inputs would result in mini-batches containing incomplete inputs (e.g., 1/4 of an image), which cannot be computed parallel to speed up inference.

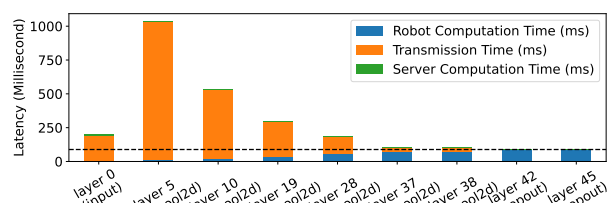
TP requires frequent synchronization among devices, leading to unacceptable communication overhead in robotic IoT.

111 By partitioning parameter tensors of a layer across GPUs,  
 112 TP allows concurrent computation on different parts of this  
 113 tensor but requires an all-reduce communication [55] to  
 114 combine computation results from different devices, which  
 115 entails significant communication overhead. Consequently,  
 116 TP is used mainly for large layers that are too large to fit in  
 117 one device in data centers and require dedicated high-speed  
 118 interconnects (e.g., 400 Gbps for NVLink [21]) even within  
 119 data centers. On the contrary, robots must prioritize seam-  
 120 less mobility and primarily depend on wireless connections,  
 121 which inherently possess limited bandwidth, as described in  
 122 Sec. 2.1, making all-reduce synchronization an unacceptable  
 123 overhead (e.g., the inference time with TP was up to 143.9X  
 124 slower than local computation in Sec.2.3).

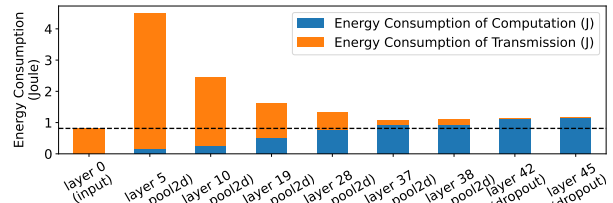
125 Consequently, existing distributed inference approaches [5,  
 126 24] in robotic IoT primarily adopt the PP paradigm and fo-  
 127 cuses on layer partitioning of PP, aiming to achieve fast and  
 128 energy-efficient inference. This is because the PP paradigm  
 129 in data centers consists of layer partitioning and pipeline  
 130 execution, where the pipeline execution of PP enhances infer-  
 131 ence throughput rather than reducing the completion time of  
 132 a single inference [6], which is the most critical requirement  
 133 in robotic IoT. Based on the fact that the amounts of output  
 134 data in some intermediate layers of a DNN model are sig-  
 135 nificantly smaller than that of its raw input data [16], DNN  
 136 layer partitioning strategies constitute various trade-offs be-  
 137 tween computation and transmission, taking into account  
 138 application-specific inference speed requirements and en-  
 139 ergy consumption demands, as shown in Fig. 1.

140 However, existing methods based on PP face significant  
 141 transmission bottlenecks in robotic IoT due to the inherent  
 142 scheduling mechanism. PP paradigm on robotic IoT consists  
 143 of three sequential phases: computing earlier DNN layers  
 144 on robots, transmitting intermediate results, and completing  
 145 inference on the GPU server. Despite optimal layer parti-  
 146 tioning strategies from [5, 24], the transmission overhead  
 147 becomes a substantial bottleneck due to limited bandwidth  
 148 of robotic IoT, accounting for up to 69% of inference time  
 149 in our experiments. While pipeline execution can mitigate  
 150 this overhead by overlapping computation and transmis-  
 151 sion phases across multiple inference tasks, it cannot reduce  
 152 the completion time of a single inference task [6], which is  
 153 crucial for robotic applications. Furthermore, the prolonged  
 154 transmission phase not only slows down inference speed but  
 155 also consumes significantly more energy.

156 The key reason for the problem of the above methods is  
 157 that existing methods conduct layer-granulated scheduling,  
 158 which prevents overlapping the transmission and computa-  
 159 tion phases within the same inference task. As transmission  
 160 time constitutes a substantial portion of the total inference  
 161 time (approximately half) in existing methods, a novel par-  
 162 allel method with finer granularity that overlaps computation  
 163 and transmission within the same inference task has the



(a) Inference Latency



(b) Energy consumption on robot

174 **Figure 1.** Existing distributed inference approaches on  
 175 VGG19 [40] in our experiments, which adopt PP paradigm  
 176 with various layer partitioning scheduling strategies. The  
 177 X-axis of the graph represents different layer partitioning  
 178 strategies, where ‘layer i’ indicates that all layers up to and  
 179 including the i-th layer are computed on the robot, while the  
 180 subsequent layers are processed on the GPU server.

181 potential to address this shortcoming, achieving fast and  
 182 energy-efficient inferences. Note that the robot can not enter  
 183 low-power sleep mode during the transmission phase due to  
 184 the need to promptly continue working upon receiving infer-  
 185 ence results, but can only enter standby mode, when chips  
 186 like CPU, GPU, and memory consume non-negligible power  
 187 even when not computing (e.g., only 5% power consumption  
 188 for wireless network cards to transmit intermediate results  
 189 in our experiments). Such a parallel method would reduce  
 190 the robot’s standby time without significantly increasing  
 191 energy consumption during the computation phase, thereby  
 192 decreasing overall energy consumption.

193 In this paper, we present Intra-DP (Intra-Data Parallel), a  
 194 high performance distributed inference system optimized for  
 195 real-world robotic IoT networks. we found that calculation  
 196 of each DNN layer is done by corresponding operators (e.g.,  
 197 matrix multiplication, convolution, pooling), and operators  
 198 can be categorized into two types: local operator and global  
 199 operator, depending on whether the operators that can be  
 200 computed independently without the complete input. For  
 201 instance, (, such as the convolution kernel in the convolu-  
 202 tion layer) Such local operator are widely exist in robotic  
 203 application, especially . enable to a novel parallel method  
 204 called Local Operator Parallel (LOP).

166  
 167  
 168  
 169  
 170  
 171  
 172  
 173  
 174  
 175  
 176  
 177  
 178  
 179  
 180  
 181  
 182  
 183  
 184  
 185  
 186  
 187  
 188  
 189  
 190  
 191  
 192  
 193  
 194  
 195  
 196  
 197  
 198  
 199  
 200  
 201  
 202  
 203  
 204  
 205  
 206  
 207  
 208  
 209  
 210  
 211  
 212  
 213  
 214  
 215  
 216  
 217  
 218  
 219  
 220

The design of Intra-DP is confronted with two major challenges. The first one is how to guarantee the correctness of inference results in Intra-DP based on LOP.

The second challenge is under LOP, how to properly schedule the computation and transmission of each local operator to achieve fast and energy-efficient inference. Nonlinear optimization problem.

We implemented Intra-DP in PyTorch [37] and evaluated Intra-DP on our real-world robots under two representative real-world environments with online training application paradigms (unsupervised domain adaptation and implicit mapping and positioning, see 2). We compared Intra-DP with BSP [?], SSP [?] and a SOTA dynamic threshold method [?] (referred to as FLOWN) under different real-world robotic IoT networks environments (namely indoors and outdoors). Evaluation shows that:

- Intra-DP is fast. Intra-DP reduced inference time by 80% ~98% compared to baselines under indoors and outdoors environments.
- Intra-DP is energy-efficient. Intra-DP reduced 91% ~98% energy consumption per inference compared to baselines, due to faster inference speed and no increased power consumption against time.
- Intra-DP is robust in various robotic IoT environments. When the robotic IoT environment changed (from indoors to outdoors), Intra-DP's superior performance remained consistent.
- Intra-DP is easy to use. It took only two lines of code to apply Intra-DP to existing ML applications.

Our main contribution is Intra-DP. xxx We envision that the fast and energy-efficient inference of Intra-DP will foster the deployment of diverse robotic tasks on real-world robots in the field. Intra-DP's code is released on <https://github.com/xxx/xxx>.

In the rest of this paper, we introduce the background of this paper in Sec. 2, give an overview of Intra-DP in Sec. 3, present the detailed design of Intra-DP in Sec. 4, evaluate Intra-DP in Sec. 6, and finally conclude in Sec. 7.

## 2 background

### 2.1 Characteristics of Robotic IoT

In real-world robotic IoT scenarios, devices often navigate and move around for tasks like search and exploration. While wireless networks provide high mobility, they also have limited bandwidth. For instance, Wi-Fi 6, the most advanced Wi-Fi technology, offers a maximum theoretical bandwidth of 1.2 Gbps for a single stream [27]. However, not only the limited hardware resources on the robot can not fully play the potential of Wi-Fi 6 [53], but also the actual available bandwidth of wireless networks is often reduced in practice

due to factors such as movement of the devices [29, 36], occlusion from by physical barriers [8, 39], and preemption of the wireless channel by other devices [2, 38].

To demonstrate the instability of wireless transmission in real-world situations, we conducted a robot surveillance experiment using four-wheel robots navigating around several given points at 5-40cm/s speed in our lab (indoors) and campus garden (outdoors), with hardware and wireless network settings as described in Sec. ???. We believe our setup represents robotic IoT devices' state-of-the-art computation and communication capabilities. We saturated the wireless network connection with iperf [1] and recorded the average bandwidth capacity between these robots every 0.1s for 5 minutes.

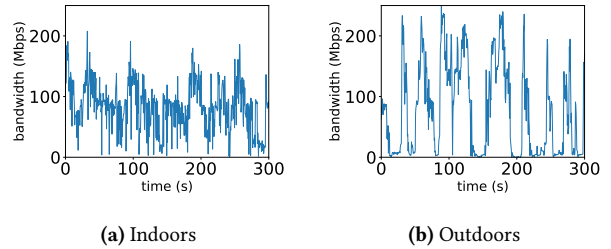


**Figure 2.** The instability of wireless transmission in robotic IoT networks.

The results in Fig. 2 show average bandwidth capacities of 93 Mbps and 73 Mbps for indoor and outdoor scenarios, respectively. The outdoor environment exhibited higher instability, with bandwidth frequently dropping to extremely low values around 0 Mbps, due to the lack of walls to reflect wireless signals and the presence of obstacles like trees between communicating robots, resulting in fewer received signals compared to indoor environments.

In summary, robotic IoT systems' wireless transmission is constrained by limited bandwidth, both due to the theoretical upper limit of wireless transmission technologies and the practical instability of wireless networks.

Notice that Only models with limited transmission overhead can mitigate the impact of these shortcomings on inference performance. However, the unstable bandwidth in robotic IoT wireless networks can cause the transmission time for layer partitioning to vary dramatically, sometimes changing by hundreds of times (see Fig. 2). In our experiments, even a relatively small model with only 0.84M parameters still suffers from its significant transmission overhead. The significant impact of transmission overhead on both inference time and energy consumption highlights the need for innovative approaches that can effectively mitigate the transmission bottleneck in robotic IoT

## 331 2.2 Characteristics of Data Center Networks

332 Data center networks, which are used for large model inference (e.g., ChatGPT [48]), are wired and typically exhibit  
 333 higher bandwidth capacity and lower fluctuation compared  
 334 to robotic IoT networks. GPU devices in data centers are  
 335 interconnected using high-speed networking technologies  
 336 such as InfiniBand [43] or PCIe [21], offering bandwidths  
 337 ranging from 40 Gbps to 500 Gbps. The primary cause of  
 338 bandwidth fluctuation in these networks is congestion on  
 339 intermediate switches, which can be mitigated through traf-  
 340 fic scheduling techniques implemented on the switches [33].  
 341 The stable and high-bandwidth nature of data center net-  
 342 works makes them well-suited for demanding tasks like  
 343 large model inference, in contrast to the more variable and  
 344 resource-constrained environments found in robotic IoT net-  
 345 works.  
 346

## 348 2.3 Existing distributed inference strategies in the 349 data center

351 **Data parallelism.** Data parallelism [50] is a widely used  
 352 technique in distributed inference that partitions input data  
 353 across multiple devices, such as GPUs, to perform parallel  
 354 inference. Each device maintains a complete model replica  
 355 and independently processes a subset of the input data (mini-  
 356 batch), aggregating results to generate the final output. Data  
 357 parallelism enhances throughput by distributing workload  
 358 across devices, leveraging their combined computational  
 359 power.

360 However, data parallelism's scalability is constrained by  
 361 the total batch size [32], which is particularly problematic  
 362 in robotic IoT applications where smaller batch sizes are  
 363 inherent due to the need for swift environmental responses.  
 364 In robotic applications, immediate inference upon receiving  
 365 inputs is crucial for obtaining real-time target points quickly.  
 366 For example, in our experiments, the robot constantly obtains  
 367 the latest images from the camera for inference, with a batch  
 368 size of only 1. These small batches cannot be further split  
 369 into mini-batches, a fundamental requirement for effective  
 370 data parallelism.

371 **Tensor parallelism.** Tensor parallelism [55] is a dis-  
 372 tributed inference technique that divides a model's layer  
 373 parameters across multiple devices, each storing and com-  
 374 puting a portion of the weights. This approach requires an  
 375 all-reduce communication step after each layer to combine  
 376 results from different devices, introducing significant over-  
 377 head, especially for large DNN layers. To mitigate this, TP is  
 378 typically deployed across GPUs within the same server in  
 379 data centers, using fast intra-server GPU-to-GPU links like  
 380 NVLink [21], which is beneficial when the model is too large  
 381 for a single device.

383 In contrast to data center networks, the limited bandwidth  
 384 in robotic IoT (see Sec. 2.1) renders the communication cost  
 385

386 of TP prohibitively high. Our experiments demonstrate that  
 387 the all-reduce communication cost of TP can consume up to  
 388 94% of the total inference time, leading to a upper to 143.9x  
 389 increase in inference time and 62.7x higher energy consump-  
 390 tion per inference compared to computing the entire model  
 391 locally on the robot (see Sec.??). Such significant overhead in-  
 392 troduced by TP's communication requirements makes it im-  
 393 practical for deployment in bandwidth-constrained robotic  
 394 IoT environments.

395 We chose a state-of-the-art tensor parallelism method,  
 396 DINA [31], as our baseline; Table 1 reveals that transmission  
 397 time constitutes 49% to 94% of total inference time due to  
 398 all-reduce communication for each layer, resulting in TP's in-  
 399 ference time being 45.2X to 143.9X longer than local computa-  
 400 tion. Although Table 2 indicates lower power consumption  
 401 with TP (13.4% to 67.3% less than local computation, because  
 402 TP spent much more time on transmission when have lower  
 403 power consumption in Tab.3), the extended transmission  
 404 times significantly increase energy consumption per infer-  
 405 ence, ranging from 28.5X to 62.7X. Since TP significantly  
 406 extends inference time, making it impractical for real-world  
 407 robotic applications that require real-time control, we did  
 408 not further evaluate TP in these contexts.

409 **Pipeline parallelism.** Pipeline parallelism [17] is a dis-  
 410 tributed inference technique that partitions DNN model lay-  
 411 ers across multiple devices(layer partitioning), forming an in-  
 412 ference pipeline for concurrent processing of multiple tasks.  
 413 While PP can increase throughput and resource utilization  
 414 via pipeline execution, it primarily focuses on enhancing  
 415 overall throughput rather than reducing single-inference la-  
 416 tency [6], which is crucial in robotic IoT. As a result, existing  
 417 distributed inference approaches [5, 24] in robotic IoT mainly  
 418 concentrate on the layer partitioning aspect of PP, aiming to  
 419 achieve fast and energy-efficient inference by optimizing the  
 420 allocation of DNN layers across devices while considering  
 421 factors such as device capabilities, network bandwidth, and  
 422 energy consumption, as discussed further in Sec. 3.1.

## 424 2.4 Other methods to speed up DNN Models 425 Inference on Robotic IoT

426 **Compressed communication.** Compressed communica-  
 427 tion is crucial for efficient distributed inference in wireless  
 428 networks, as it significantly reduces communication over-  
 429 head through techniques such as quantization and model  
 430 distillation. Quantization [7, 11, 12] is a technique that re-  
 431 duces the numerical precision of model weights and ac-  
 432 tivations, thereby minimizing the memory footprint and  
 433 computational requirements of deep learning models. This  
 434 process typically involves converting high-precision (e.g.,  
 435 32-bit) floating-point values to lower-precision (e.g., 8-bit)  
 436 floating-point representations, with minimal loss of model  
 437 accuracy. Model distillation [13, 26, 45], on the other hand,  
 438

Model(number of parameters)	Local computation time(s)	Environment	Transmission time (s) with TP	Inference time (s) with TP	Percentage(%) with TP
MobileNet_V3_Small(2M)	0.031( $\pm 0.004$ )	indoors	0.698( $\pm 0.135$ )	1.400( $\pm 0.232$ )	49.85
		outdoors	0.901( $\pm 0.778$ )	1.775( $\pm 1.370$ )	51.23
ResNet101(44M)	0.065( $\pm 0.005$ )	indoors	7.156( $\pm 3.348$ )	8.106( $\pm 3.403$ )	87.95
		outdoors	8.470( $\pm 6.337$ )	9.356( $\pm 6.328$ )	90.46
VGG19_BN(143M)	0.063( $\pm 0.002$ )	indoors	5.152( $\pm 4.873$ )	5.444( $\pm 4.831$ )	70.18
		outdoors	5.407( $\pm 6.673$ )	5.759( $\pm 6.635$ )	93.70

**Table 1.** Average transmission time (Second), inference time (Second), percentage that transmission time accounts for of inference time and their standard deviation ( $\pm n$ ) with TP on different models in different environments. “Local computation” refers to placing the whole layers on the robot.

Model(number of parameters)	Environment	Power consumption(W)		Energy consumption(J) per inference	
		Local	TP	Local	TP
MobileNet_V3_Small(2M)	indoors	6.05( $\pm 0.21$ )	5.24( $\pm 0.19$ )	0.3( $\pm 0.09$ )	7.33( $\pm 1.21$ )
	outdoors	6.05( $\pm 0.21$ )	5.11( $\pm 0.28$ )	0.3( $\pm 0.09$ )	9.08( $\pm 7.0$ )
ResNet101(44M)	indoors	11.27( $\pm 0.51$ )	4.97( $\pm 0.16$ )	0.93( $\pm 0.19$ )	40.28( $\pm 16.91$ )
	outdoors	11.27( $\pm 0.51$ )	4.9( $\pm 0.23$ )	0.93( $\pm 0.19$ )	45.8( $\pm 30.98$ )
VGG19_BN(143M)	indoors	14.86( $\pm 0.43$ )	4.88( $\pm 0.29$ )	1.19( $\pm 0.18$ )	26.55( $\pm 23.56$ )
	outdoors	14.86( $\pm 0.43$ )	4.87( $\pm 0.27$ )	1.19( $\pm 0.18$ )	28.06( $\pm 32.33$ )

**Table 2.** Power consumption against time (Watt) and energy consumption per inference (Joule) with standard deviation ( $\pm n$ ) with TP on different models in different environments. “Local” represents “Local computation”

is an approach that involves training a smaller, more efficient “student” model to mimic the behavior of a larger, more accurate “teacher” model by minimizing the difference between the student model’s output and the teacher model’s output. The distilled student model retains much of the teacher model’s accuracy while requiring significantly fewer resources. These model compression methods complement distributed inference by achieving faster inference speed through model modifications, potentially sacrificing some accuracy with smaller models, while distributed inference realizes fast inference without loss of accuracy by intelligently scheduling computation tasks across multiple devices. Moreover, given the requirement to maintain the integrity of the final inference results, intermediate results cannot be altered during transmission. Consequently, only lossless compression methods [14] can be utilized to reduce the transmission volume.

**Inference Job scheduling.** Significant research efforts have been devoted to exploring inference parallelism and unleashing the potential of layer partition to accelerate DNN inference, such as inference job scheduling, aiming to accelerate multiple DNN inference tasks by optimizing their execution on various devices under different network bandwidths while considering application-specific inference speed requirements and energy consumption demands. For instance, [3, 9] support online scheduling of offloading inference tasks based on the current network and resource status of mobile systems while meeting user-defined energy constraints. [10] focused on optimizing DNN inference workloads in cloud

computing using a deep reinforcement learning based scheduler for QoS-aware scheduling of heterogeneous servers, aiming to maximize inference accuracy and minimize response delay. While these methods focus on overall optimization in multi-task scenarios involving multi-robots, they do not address the optimization of single inference tasks and are thus orthogonal to distributed inference for a single inference, where improved distributed inference can provide faster and more energy-efficient inference for these scenarios.

### 3 Overview

#### 3.1 Existing distributed inference on robotic IoT

Existing distributed inference approaches [5, 24] in robotic IoT primarily adopt the PP paradigm and focus on layer partitioning to achieve fast and energy-efficient inference. These approaches can be divided into two main categories based on their optimization goals: accelerating inference for diverse DNN structures and optimizing robot energy consumption during inference.

To accelerate inference, earlier methods [16, 19, 31] focused on simple chain-like DNN models by exploiting the smaller output data sizes of intermediate layers compared to raw input data [16], creating trade-offs between computation and transmission to minimize overall inference time (see Fig. 1). However, the increasing complexity of DNN structures, now evolved into directed acyclic graphs (DAGs), poses new challenges, potentially leading to NP-hardness in performance optimization [24]. This issue is addressed by

graph theory techniques [24, 52] and varying hardware and network conditions further complicate the problem.

To optimize energy consumption, existing methods [5, 25, 47] build upon the aforementioned techniques and consider reducing the system energy consumption of the entire layer partitioning execution process under deadline constraints. While [47] only considers transmission energy consumption, [5, 25] aim to reduce the whole system's energy consumption during DNN layer execution and data transfer.

In summary, these two categories primarily adopt the PP paradigm but suffer from the transmission bottleneck inherent to PP's scheduling mechanism (see Sec. 3.2). Consequently, achieving fast and energy-efficient inference on robotic IoT remains an open issue.

### 3.2 Dilemma on Inference Time and Energy Consumption

Regardless of the complexity of DNN models, layer partitioning methods consist of three phases: computing earlier DNN layers on robots, transmitting intermediate results, and completing inference on the GPU device. Since the GPU device's computation time is negligible compared to the other two phases (see Fig. 1) due to the high computing capabilities of GPU devices, this paper focuses on the computation phase of robots and the data transmission phase via robotic IoT.

The data transmission phase can only begin after obtaining the calculation result of the intermediate layer when the computation phase on robots is completed, preventing overlap for a single inference task. PP can only overlap computation and data transmission phases from different inference tasks, not from the same task [6]. However, the transmission cost inherent to the PP's scheduling mechanism becomes a bottleneck in robotic IoT due to limited bandwidth. In our experiments, even with optimal layer partitioning [5, 24], such communication cost takes up to 63% of inference time.

To make matters worse, such transmission overhead not only leads to prolonged inference time but also to high energy consumption during the data transmission phase, referred to as transmission energy consumption. Our findings reveal that such transmission energy consumption accounts for nearly one-third of the total energy consumed during inference (see Sec. ??). This is because the device cannot be put into low-power sleep mode while waiting for the final inference result from the GPU device, as it has to promptly continue working when it receives the inference results. Moreover, chips like CPU, GPU, and memory consume non-negligible power even when not computing, due to the static power consumption rooted in transistors' leakage current [20]. Consequently, both the energy consumed during the execution of DNN layers on robots, referred to as robot computation energy consumption, and the transmission energy consumption resulting from prolonged transmission

times substantially impact the overall power consumption of the inference process in robotic IoT.

Only models with limited transmission overhead can mitigate the impact of these shortcomings on inference performance. However, the unstable bandwidth in robotic IoT wireless networks can cause the transmission time for layer partitioning to vary dramatically, sometimes changing by hundreds of times (see Fig. 2). In our experiments, even a relatively small model with only 0.84M parameters still suffers from its significant transmission overhead. The significant impact of transmission overhead on both inference time and energy consumption highlights the need for innovative approaches that can effectively mitigate the transmission bottleneck in robotic IoT.

### 3.3 Special Cases

Since layer partitioning methods schedule at the granularity of model layers, “local computation” and “edge computation” are special cases of layer partitioning. “Local computation” refers to placing the whole layers on the robot when the bandwidth is too low, while “edge computation” means placing the whole layers on GPU devices when the bandwidth is sufficient. Local computation avoids the impact of network transmission on inference time but consumes the maximum computation energy consumption. On the other hand, edge computation minimizes computation energy consumption but requires a high enough bandwidth to ensure the lowest possible transmission energy consumption and overall inference time. These two special cases are indispensable for existing methods to cope with different network conditions, when they are too low or sufficient, and to address the need for various trade-offs between inference delay and energy consumption.

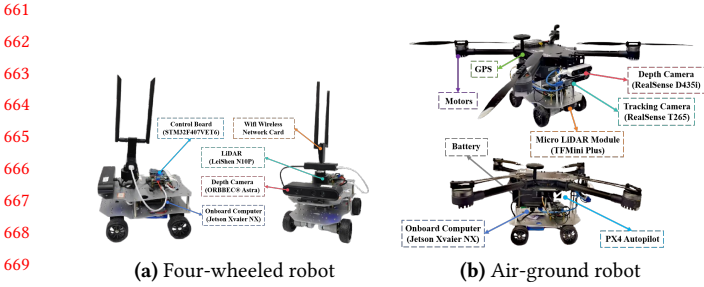
In our experiments, we found that the bandwidth conditions under which the layer partitioning scheme of different models becomes these special cases vary, and the higher the bandwidth, the more layers are scheduled to be placed on GPU devices. We explain the reasons causing different bandwidth conditions for different models in Sec. ?? with some detailed real-world cases. The existence of these special cases highlights the importance of considering the relationship between bandwidth, model structure, and the resulting trade-offs between inference delay and energy consumption.

## 4 Detailed Design

## 5 Implementation

## 6 Evaluation

**Testbed.** The evaluation was conducted on a custom four-wheeled robot (Fig 3a), and a custom air-ground robot (Fig 3b). They are equipped with a Jetson Xavier NX [34] 8G onboard computer that is capable of AI model inference with local computation resources. The system runs Ubuntu 20.04 with

**Figure 3.** The detailed composition of the robot platforms

	inference	transmission	standby
Power (W)	13.35	4.25	4.04

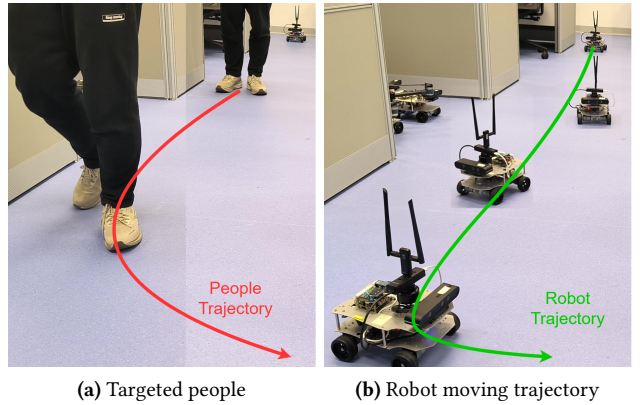
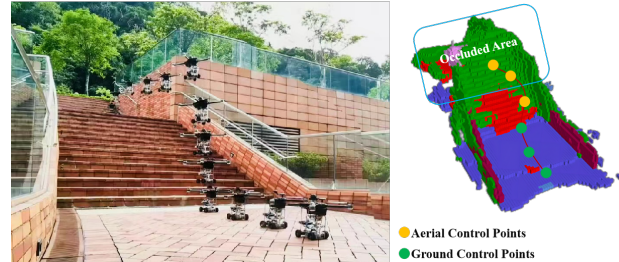
**Table 3.** Power consumption (Watt) of our robot in different states.

ROS Noetic and a dual-band USB network card (MediaTek MT76x2U) for wireless connectivity. The Jetson Xavier NX interfaces with a Leishen N10P LiDAR, ORBBEC Astra depth camera, and an STM32F407VET6 controller via USB serial ports. Both LiDAR and depth cameras facilitate environmental perception, enabling autonomous navigation, obstacle avoidance, and SLAM mapping. The GPU server accepting offloaded computation tasks from the robot is a PC equipped with an Intel(R) i5 12400f CPU @ 4.40GHz and an NVIDIA GeForce GTX 2080 Ti 11GB GPU, connected to our robot via Wi-Fi 6 over 80MHz channel at 5GHz frequency in our experiments.

Tab. 3 presents the overall on-board energy consumption (excluding motor energy consumption for robot movement) of the robot in various states: inference (model inference with full GPU utilization, including CPU and GPU energy consumption), transmission (communication with the GPU server, including wireless network card energy consumption), and standby (robot has no tasks to execute). Notice that different models, due to varying numbers of parameters, exhibit distinct GPU utilization rates and power consumption during inference.

**Experiment Environments.** We evaluated two real-world environments: indoors (robots move in our laboratory with desks and separators interfering with wireless signals) and outdoors (robots move in our campus garden with trees and bushes interfering with wireless signals, resulting in lower bandwidth). The corresponding bandwidths between the robot and the GPU server in indoors and outdoors scenarios are shown in Fig. 2.

**Workload.** We evaluated two typical real-world robotic applications on our testbed: Kapao, a real-time people-tracking application on our four-wheeled robot (Fig 4), and AGRNav, an autonomous navigation application on our air-ground robot (Fig 5). These applications feature different model input and output size patterns: Kapao takes RGB images as input

**Figure 4.** A real-time people-tracking robotic application on our robot based on a well-known human pose estimation ML model, Kapao [30].**Figure 5.** By predicting occlusions in advance, AGRNav [44] gains an accurate perception of the environment and avoids collisions, resulting in efficient and energy-saving paths.

and outputs key points of small data volume. In contrast, AGRNav takes point clouds as input and outputs predicted point clouds and semantics of similar data volume as input, implying that AGRNav needs to transmit more data during offloading. And we have verified several models common to mobile devices on a larger scale to further corroborate our observations and findings: MobileNet [41], ResNet [42], VGGNet [40], ConvNeXt [46], RegNet [51].

**Baselines.** We selected two SOTA pipeline parallelism methods as baselines: DSCCS [24], aimed at accelerating inference, and SPSO-GA [5], focused on optimizing energy consumption. We set SPSO-GA's deadline constraints to 1 Hz, the minimum frequency required for robot movement control. Given our primary focus on inference time and energy consumption per inference, we disabled pipeline execution to concentrate solely on assessing the performance of various layer partitioning methods.

## 6.1 Inference Time

**Kapao.** From the results in the upper part of Tab. 4, both SPSO-GA and DSCCS reduced Kapao's inference time by 39.69% and 56.92% indoors and 28.67% and 47.46% outdoors,

Model(number of parameters)	Local com- putation time (s)	Environment	Transmission time (s)			Inference time (s)		
			DSCCS	SPSO-GA	Intra-DP	DSCCS	SPSO-GA	Intra-DP
kapao(77M)	0.0( $\pm 0.0$ )	indoors	0.228( $\pm 0.176$ )	0.235( $\pm 0.164$ )	0.259( $\pm 0.181$ )	0.343( $\pm 0.192$ )	0.311( $\pm 0.168$ )	0.264( $\pm 0.166$ )
		outdoors	0.087( $\pm 0.178$ )	0.35( $\pm 1.045$ )	0.385( $\pm 1.15$ )	0.696( $\pm 0.125$ )	0.434( $\pm 1.046$ )	0.369( $\pm 0.125$ )
agrnav(0M)	0.0( $\pm 0.0$ )	indoors	0.266( $\pm 0.166$ )	0.239( $\pm 0.149$ )	0.263( $\pm 0.164$ )	0.433( $\pm 0.134$ )	0.427( $\pm 0.12$ )	0.365( $\pm 0.134$ )
		outdoors	0.263( $\pm 0.843$ )	0.218( $\pm 0.796$ )	0.24( $\pm 0.875$ )	0.512( $\pm 0.779$ )	0.536( $\pm 0.72$ )	0.456( $\pm 0.72$ )

**Table 4.** Average transmission time (Second), inference time (Second), percentage that transmission time accounts for of inference time and their standard deviation ( $\pm n$ ) of Kapao and AGRNav with different pipeline parallelism offloading systems and different environments. “Local computation” refers to placing the whole layers on the robot.

Model(number of parameters)	Environment	Power consumption(W)			Energy consumption(J) per inference			
		Local	DSCCS	SPSO-GA	Intra-DP	Local	DSCCS	SPSO-GA
kapao(77M)	indoors	15.04( $\pm 0.64$ )	7.03( $\pm 3.57$ )	5.92( $\pm 2.18$ )	5.03( $\pm 1.87$ )	15.03( $\pm 0.63$ )	2.41( $\pm 1.35$ )	1.84( $\pm 1.0$ )
	outdoors	15.04( $\pm 0.64$ )	14.15( $\pm 1.71$ )	5.89( $\pm 2.3$ )	5.02( $\pm 1.97$ )	1.56( $\pm 0.85$ )	9.85( $\pm 1.77$ )	2.56( $\pm 6.17$ )
agrnav(0.84M)	indoors	10.26( $\pm 1.58$ )	6.6( $\pm 1.95$ )	6.74( $\pm 2.03$ )	5.74( $\pm 1.78$ )	10.82( $\pm 1.44$ )	2.86( $\pm 0.88$ )	2.88( $\pm 0.81$ )
	outdoors	10.26( $\pm 1.58$ )	7.36( $\pm 2.34$ )	7.91( $\pm 2.45$ )	6.71( $\pm 2.1$ )	10.82( $\pm 1.44$ )	3.77( $\pm 5.74$ )	4.25( $\pm 5.7$ )

**Table 5.** The power consumption against time (Watt) and energy consumption per inference (Joule) with standard deviation ( $\pm n$ ) of Kapao and AGRNav at different baselines and environments. “Local” represents “Local computation”

with DSCCS achieving 28.57% (indoors) and 26.34% (outdoors) lower inference time than SPSO-GA. While both systems significantly reduced inference time via offloading, transmission time accounts for 49.69% to 69.46% of the whole inference time, indicating that even with SOTA layer partitioning, the transmission bottleneck inherent to PP’s scheduling mechanism cannot be mitigated. The difference between DSCCS and SPSO-GA can be attributed to their optimization goals: DSCCS minimizes inference latency, while SPSO-GA minimizes power consumption under deadline constraints.

**AGRNav.** The performance gain of the two offloading systems varied for AGRNav, as shown in the lower part of Tab. 4. DSCCS still reduced inference time by 18.34% and 12.43% in indoors and outdoors. However, SPSO-GA achieved similar inference time (3.65% and 3.06% reduction) as local computation both indoors and outdoors. We will explain and analyze this phenomenon in Sec.6.2.

Notice that the large standard deviation in transmission time in outdoors in both offloading systems indicates that bandwidth fluctuated more frequently and more fiercely outdoors compared with indoors, which complies with Fig. 2. Additionally, the lower average bandwidth for outdoors scenarios (see Sec.2.1) results in increased transmission and inference times relative to indoor scenarios.

## 6.2 Breakdown

Both SPSO-GA and DSCCS automatically adapt to available bandwidth, transitioning to edge computation (placing all DNN layers on the GPU server) when bandwidth is sufficient, and to local computation (placing all DNN layers on robots) when bandwidth is low. To better understand how their layer partitioning scheduling varies with different network conditions and models, we recorded and analyzed the

Categories and percentages of various layer partitioning schedules under different baselines and environments, as detailed in Fig. 6.

Local computation and edge computation are special cases of layer partitioning, with the bandwidth conditions required for each model to reach these cases varying based on the model structure and partitioning method used. Analyzing Fig. 6a and Fig. 6b, both SPSO-GA and DSCCS tend to allocate more layers on the robot for AGRNav. When comparing indoor and outdoor scenarios in Fig. 6, it is evident that higher bandwidth leads to more layers being scheduled on GPU server. Additionally, when comparing SPSO-GA and DSCCS in Fig. 6, DSCCS, which focuses on optimizing energy consumption, tends to place fewer layers on the robot to reduce computation energy consumption.

In summary, the conditions under which layer partitioning schemes make these special cases are influenced by multiple factors: model structure, and the trade-offs between inference delay and energy consumption. And the higher the bandwidth, the more layers are scheduled to be placed on GPU server.

## 6.3 Energy Consumption

**Kapao.** From the results in the upper part of Tab. 5, DSCCS consumed 3.38% and 2.02% more power per second than SPSO-GA indoors and outdoors due to more layers placed on robots shown in Fig. 6a. However, SPSO-GA consumed 58.54% and 49.74% more energy overall to process a frame than DSCCS because it only aims at minimizing the power consumption against time at the cost of possibly prolonged inference time.

Model(number of parameters)	Local computation time (s)	Environment	Transmission time (s)		Inference time (s)		Percentage(%)	
			SPSO-GA	DSCCS	SPSO-GA	DSCCS	SPSO-GA	DSCCS
MobileNet_V3_Small (2M)	0.033(±0.019)	indoors	0.035(±0.019)	0.016(±0.005)	0.044(±0.020)	0.031(±0.008)	79.79	53.24
		outdoors	0.035(±0.044)	0.017(±0.005)	0.047(±0.037)	0.033(±0.018)	50.04	51.49
RegNet_X_3_2GF (15M)	0.060(±0.022)	indoors	0.049(±0.026)	0.033(±0.011)	0.065(±0.028)	0.049(±0.016)	76.25	64.17
		outdoors	0.049(±0.055)	0.032(±0.032)	0.069(±0.050)	0.051(±0.030)	53.23	44.50
ResNet101 (44M)	0.060(±0.023)	indoors	0.054(±0.451)	0.033(±0.010)	0.072(±0.453)	0.050(±0.016)	75.64	57.37
		outdoors	0.052(±0.064)	0.033(±0.036)	0.077(±0.059)	0.054(±0.034)	51.54	42.48
ConvNeXt_Base (88M)	0.047(±0.004)	indoors	0.033(±0.018)	0.020(±0.006)	0.044(±0.019)	0.032(±0.009)	75.39	49.37
		outdoors	0.032(±0.038)	0.020(±0.022)	0.045(±0.033)	0.034(±0.019)	52.82	35.63
ConvNeXt_Large (197M)	0.051(±0.005)	indoors	0.033(±0.017)	0.023(±0.008)	0.046(±0.019)	0.035(±0.013)	72.96	62.68
		outdoors	0.032(±0.038)	0.023(±0.024)	0.054(±0.040)	0.041(±0.028)	48.94	43.96
RegNet_Y_128GF (644M)	0.139(±0.016)	indoors	0.076(±0.289)	0.041(±0.024)	0.305(±0.382)	0.100(±0.035)	23.58	40.76
		outdoors	0.171(±0.602)	0.016(±0.055)	0.432(±0.615)	0.117(±0.242)	32.39	9.41

**Table 6.** Average transmission time (Second), inference time (Second), percentage that transmission time accounts for of inference time and their standard deviation ( $\pm n$ ) of common AI models in different environments with different offloading systems. “Local computation” refers to placing the whole layers on the robot.

Model(number of parameters)	Environment	Power consumption(W)			Energy consumption(J) per inference		
		Local	SPSO-GA	DSCCS	Local	SPSO-GA	DSCCS
MobileNet_V3_Small (2M)	indoors	6.131(±0.061)	5.448(±0.168)	5.658(±0.085)	0.202(±0.002)	0.241(±0.107)	0.174(±0.046)
	outdoors	6.131(±0.061)	5.567(±0.273)	5.557(±0.186)	0.202(±0.002)	0.260(±0.204)	0.185(±0.099)
RegNet_X_3_2GF (15M)	indoors	8.208(±0.140)	5.490(±0.178)	5.714(±0.342)	0.492(±0.008)	0.356(±0.156)	0.278(±0.058)
	outdoors	8.208(±0.140)	5.878(±0.659)	6.041(±0.624)	0.492(±0.008)	0.406(±0.295)	0.311(±0.184)
ResNet101 (44M)	indoors	11.851(±0.404)	5.457(±0.240)	5.953(±0.789)	0.711(±0.024)	0.390(±2.471)	0.298(±0.094)
	outdoors	11.851(±0.404)	6.179(±1.083)	6.431(±1.060)	0.711(±0.024)	0.478(±0.364)	0.349(±0.216)
ConvNeXt_Base (88M)	indoors	15.335(±0.273)	5.507(±0.358)	7.713(±2.613)	0.721(±0.013)	0.241(±0.103)	0.250(±0.069)
	outdoors	15.335(±0.273)	7.638(±3.297)	9.148(±3.338)	0.721(±0.013)	0.346(±0.254)	0.307(±0.171)
ConvNeXt_Large (197M)	indoors	15.403(±0.082)	5.518(±0.638)	6.604(±2.860)	0.786(±0.004)	0.251(±0.104)	0.230(±0.088)
	outdoors	15.403(±0.082)	8.400(±4.345)	8.895(±4.505)	0.786(±0.004)	0.452(±0.339)	0.366(±0.248)
RegNet_Y_128GF (644M)	indoors	15.430(±0.020)	5.384(±1.071)	6.151(±2.155)	2.145(±0.003)	1.642(±0.327)	0.615(±0.216)
	outdoors	15.430(±0.020)	6.361(±2.349)	9.127(±4.724)	2.145(±0.003)	2.748(±1.015)	1.068(±0.553)

**Table 7.** The power consumption against time (Watt) and energy consumption per inference (Joule) with standard deviation ( $\pm n$ ) of common AI models at different baselines and environments. “Local” represents “Local computation”

**AGRNav.** From the results in the lower part of Tab. 5, DSCCS consumed 61.21% and 22.92% more energy per second than SPSO-GA indoors and outdoors ( Tab. 5), while DSCCS consumed 34.15% and 5.43% more energy to process a frame than SPSO-GA. SPSO-GA’s advantages in power consumption against time shrinks in energy consumption per inference due to prolonged inference time.

#### 6.4 Validation on a larger range of models

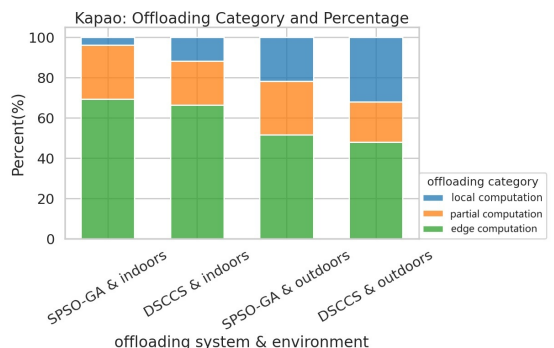
We evaluated PP across a broad range of models with varying parameter counts (from 0.84M to 644M, as detailed in Tab. 6 and Tab. 7), which are commonly used in mobile devices. Our findings confirm that transmission time constitutes a significant portion of the total inference time in robotic IoT when using PP. The inherent transmission overhead of PP’s scheduling mechanism significantly wastes both inference time and energy.

## 7 Conclusion

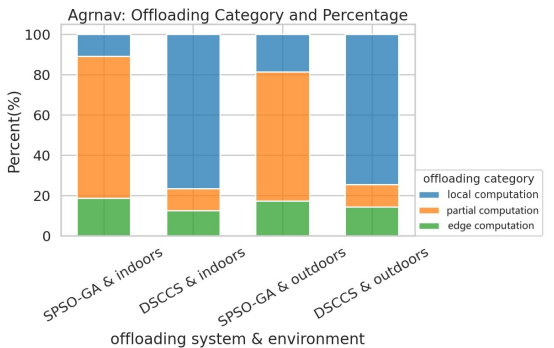
In this paper, we explored the problems that hinder the application of existing parallel methods for distributed inference on robotic IoT, including the failure of data parallelism due to small batch sizes, the unacceptable communication overhead of tensor parallelism caused by all-reduce communication, and the significant transmission bottlenecks inherent to pipeline parallelism’s scheduling mechanism. By raising awareness of these issues, we aim to stimulate research efforts towards developing novel parallel methods that address these problems. We envision that fast and energy-efficient inference will foster the deployment of diverse robotic tasks on real-world robots in the field.

## References

- [1] [n. d.]. iPerf - Download iPerf3 and original iPerf pre-compiled binaries. <https://iperf.fr/iperf-download.php>



(a) Categories and percentage of various scheduling for Kapao



(b) Categories and percentage of various scheduling for AGRNav

**Figure 6.** The layer partitioning scheduling under different baselines and environments. “Local computation” refers to placing the whole layers on the robot when the bandwidth is too low, “edge computation” means placing the whole layers on GPU server when the bandwidth is sufficient, and “partial computation” means placing part of the layers on the robot and part on GPU server.

- [2] Toni Adame, Marc Carrascosa-Zamacois, and Boris Bellalta. 2021. Time-sensitive networking in IEEE 802.11 be: On the way to low-latency WiFi 7. *Sensors* 21, 15 (2021), 4954.
- [3] Majid Altamimi, Atef Abdabou, Kshirasagar Naik, and Amiya Nayak. 2015. Energy cost models of smartphones for task offloading to the cloud. *IEEE Transactions on Emerging Topics in Computing* 3, 3 (2015), 384–398.
- [4] Anh-Quan Cao and Raoul de Charette. 2022. Monoscene: Monocular 3d semantic scene completion. In *Proceedings of the IEEE/CVF Conference on Computer Vision and Pattern Recognition*. 3991–4001.
- [5] Xing Chen, Jianshan Zhang, Bing Lin, Zheyi Chen, Katinka Wolter, and Geyong Min. 2021. Energy-efficient offloading for DNN-based smart IoT systems in cloud-edge environments. *IEEE Transactions on Parallel and Distributed Systems* 33, 3 (2021), 683–697.
- [6] Daniel Crankshaw, Gur-Eyal Sela, Xiangxi Mo, Corey Zumar, Ion Stoica, Joseph Gonzalez, and Alexey Tumanov. 2020. InferLine: latency-aware provisioning and scaling for prediction serving pipelines. In *Proceedings of the 11th ACM Symposium on Cloud Computing*. 477–491.
- [7] Alexandre Défossez, Yossi Adi, and Gabriel Synnaeve. 2021. Differentiable model compression via pseudo quantization noise. *arXiv preprint arXiv:2104.09987* (2021).
- [8] Ming Ding, Peng Wang, David López-Pérez, Guoqiang Mao, and Zihuai Lin. 2015. Performance impact of LoS and NLoS transmissions in dense

cellular networks. *IEEE Transactions on Wireless Communications* 15, 3 (2015), 2365–2380.

- [9] Khalid Elgazzar, Patrick Martin, and Hossam S Hassanein. 2014. Cloud-assisted computation offloading to support mobile services. *IEEE Transactions on Cloud Computing* 4, 3 (2014), 279–292.
- [10] Zhou Fang, Tong Yu, Ole J Mengshoel, and Rajesh K Gupta. 2017. Qos-aware scheduling of heterogeneous servers for inference in deep neural networks. In *Proceedings of the 2017 ACM on Conference on Information and Knowledge Management*. 2067–2070.
- [11] Stefan Gheorghe and Mihai Ivanovici. 2021. Model-based weight quantization for convolutional neural network compression. In *2021 16th International Conference on Engineering of Modern Electric Systems (EMES)*. IEEE, 1–4.
- [12] Cheng Gong, Yao Chen, Ye Lu, Tao Li, Cong Hao, and Deming Chen. 2020. VecQ: Minimal loss DNN model compression with vectorized weight quantization. *IEEE Trans. Comput.* 70, 5 (2020), 696–710.
- [13] Jianping Gou, Baosheng Yu, Stephen J Maybank, and Dacheng Tao. 2021. Knowledge distillation: A survey. *International Journal of Computer Vision* 129, 6 (2021), 1789–1819.
- [14] Apoorv Gupta, Aman Bansal, and Vidhi Khanduja. 2017. Modern lossless compression techniques: Review, comparison and analysis. In *2017 Second International Conference on Electrical, Computer and Communication Technologies (ICECCT)*. IEEE, 1–8.
- [15] Vinayak Honkote, Dileep Kurian, Sriram Muthukumar, Dibyendu Ghosh, Satish Yada, Kartik Jain, Bradley Jackson, Ilya Klotchkov, Mallikarjuna Rao Nimmagadda, Shreela Dattawadkar, et al. 2019. 2.4 a distributed autonomous and collaborative multi-robot system featuring a low-power robot soc in 22nm cmos for integrated battery-powered minibots. In *2019 IEEE International Solid-State Circuits Conference-(ISSCC)*. IEEE, 48–50.
- [16] Chuang Hu, Wei Bao, Dan Wang, and Fengming Liu. 2019. Dynamic adaptive DNN surgery for inference acceleration on the edge. In *IEEE INFOCOM 2019-IEEE Conference on Computer Communications*. IEEE, 1423–1431.
- [17] Yang Hu, Connor Imes, Xuanang Zhao, Souvik Kundu, Peter A Beerel, Stephen P Crago, and John Paul Walters. 2022. Pipeedge: Pipeline parallelism for large-scale model inference on heterogeneous edge devices. In *2022 25th Euromicro Conference on Digital System Design (DSD)*. IEEE, 298–307.
- [18] KJ Joseph, Salman Khan, Fahad Shahbaz Khan, and Vineeth N Balasubramanian. 2021. Towards Open World Object Detection. In *Proceedings of the IEEE/CVF Conference on Computer Vision and Pattern Recognition (CVPR)*. 5830–5840.
- [19] Yiping Kang, Johann Hauswald, Cao Gao, Austin Rovinski, Trevor Mudge, Jason Mars, and Lingjia Tang. 2017. Neurosurgeon: Collaborative intelligence between the cloud and mobile edge. *ACM SIGARCH Computer Architecture News* 45, 1 (2017), 615–629.
- [20] Nam Sung Kim, Todd Austin, David Baauw, Trevor Mudge, Krisztian Flautner, Jie S Hu, Mary Jane Irwin, Mahmut Kandemir, and Vijaykrishnan Narayanan. 2003. Leakage current: Moore’s law meets static power. *computer* 36, 12 (2003), 68–75.
- [21] Ang Li, Shuaiwen Leon Song, Jieyang Chen, Jiajia Li, Xu Liu, Nathan R Tallent, and Kevin J Barker. 2019. Evaluating modern gpu interconnect: Pcie, nvlk, nv-sli, nvswitch and gpudirect. *IEEE Transactions on Parallel and Distributed Systems* 31, 1 (2019), 94–110.
- [22] Qingbiao Li, Fernando Gama, Alejandro Ribeiro, and Amanda Prorok. 2020. Graph neural networks for decentralized multi-robot path planning. In *2020 IEEE/RSJ International Conference on Intelligent Robots and Systems (IROS)*. IEEE, 11785–11792.
- [23] Yiming Li, Zhiding Yu, Christopher Choy, Chaowei Xiao, Jose M Alvarez, Sanja Fidler, Chen Feng, and Anima Anandkumar. 2023. Voxformer: Sparse voxel transformer for camera-based 3d semantic scene completion. In *Proceedings of the IEEE/CVF Conference on Computer Vision and Pattern Recognition*. 9087–9098.

1046  
1047  
1048  
1049  
1050  
1051  
1052  
1053  
1054  
1055  
1056  
1057  
1058  
1059  
1060  
1061  
1062  
1063  
1064  
1065  
1066  
1067  
1068  
1069  
1070  
1071  
1072  
1073  
1074  
1075  
1076  
1077  
1078  
1079  
1080  
1081  
1082  
1083  
1084  
1085  
1086  
1087  
1088  
1089  
1090  
1091  
1092  
1093  
1094  
1095  
1096  
1097  
1098  
1099  
1100

- 1101 [24] Huanghuang Liang, Qianlong Sang, Chuang Hu, Dazhao Cheng, Xi-  
1102 aobo Zhou, Dan Wang, Wei Bao, and Yu Wang. 2023. DNN surgery:  
1103 Accelerating DNN inference on the edge through layer partitioning.  
1104 *IEEE transactions on Cloud Computing* (2023).
- 1105 [25] Bing Lin, Yinhao Huang, Jianshan Zhang, Junqin Hu, Xing Chen, and  
1106 Jun Li. 2019. Cost-driven off-loading for DNN-based applications  
1107 over cloud, edge, and end devices. *IEEE Transactions on Industrial  
1108 Informatics* 16, 8 (2019), 5456–5466.
- 1109 [26] Tao Lin, Lingjing Kong, Sebastian U Stich, and Martin Jaggi. 2020.  
1110 Ensemble distillation for robust model fusion in federated learning.  
1111 *Advances in Neural Information Processing Systems* 33 (2020), 2351–  
1112 2363.
- 1113 [27] Ruofeng Liu and Nakjung Choi. 2023. A First Look at Wi-Fi 6 in Action:  
1114 Throughput, Latency, Energy Efficiency, and Security. *Proceedings  
1115 of the ACM on Measurement and Analysis of Computing Systems* 7, 1  
1116 (2023), 1–25.
- 1117 [28] Shuai Liu, Xin Li, Huchuan Lu, and You He. 2022. Multi-Object Track-  
1118 ing Meets Moving UAV. In *Proceedings of the IEEE/CVF Conference on  
1119 Computer Vision and Pattern Recognition (CVPR)*. 8876–8885.
- 1120 [29] Antoni Masiukiewicz. 2019. Throughput comparison between the new  
1121 HEW 802.11 ax standard and 802.11 n/ac standards in selected distance  
1122 windows. *International Journal of Electronics and Telecommunications*  
1123 65, 1 (2019), 79–84.
- 1124 [30] William McNally, Kanav Vats, Alexander Wong, and John McPhee.  
1125 2022. Rethinking keypoint representations: Modeling keypoints and  
1126 poses as objects for multi-person human pose estimation. In *European  
1127 Conference on Computer Vision*. Springer, 37–54.
- 1128 [31] Thaha Mohammed, Carlee Joe-Wong, Rohit Babbar, and Mario  
1129 Di Francesco. 2020. Distributed inference acceleration with adaptive  
1130 DNN partitioning and offloading. In *IEEE INFOCOM 2020-IEEE  
1131 Conference on Computer Communications*. IEEE, 854–863.
- 1132 [32] Deepak Narayanan, Mohammad Shoeybi, Jared Casper, Patrick LeGresley,  
1133 Mostofa Patwary, Vijay Korthikanti, Dmitri Vainbrand, Prethvi  
1134 Kashinkunti, Julie Bernauer, Bryan Catanzaro, et al. 2021. Efficient  
1135 large-scale language model training on gpu clusters using megatron-  
1136 lm. In *Proceedings of the International Conference for High Performance  
1137 Computing, Networking, Storage and Analysis*. 1–15.
- 1138 [33] Mohammad Noormohammadpour and Cauligi S Raghavendra. 2017.  
1139 Datacenter traffic control: Understanding techniques and tradeoffs.  
1140 *IEEE Communications Surveys & Tutorials* 20, 2 (2017), 1492–1525.
- 1141 [34] NVIDIA. 2024. The World’s Smallest AI Supercomputer.  
1142 [https://www.nvidia.com/en-us/autonomous-machines/embedded-  
1143 systems/jetson-xavier-series/](https://www.nvidia.com/en-us/autonomous-machines/embedded-systems/jetson-xavier-series/).
- 1144 [35] Takeshi Ohkawa, Kazushi Yamashina, Hitomi Kimura, Kanemitsu  
1145 Ootsu, and Takashi Yokota. 2018. FPGA components for integrating  
1146 FPGAs into robot systems. *IEICE TRANSACTIONS on Information and  
1147 Systems* 101, 2 (2018), 363–375.
- 1148 [36] Yuanteng Pei, Matt W Mutka, and Ning Xi. 2013. Connectivity and  
1149 bandwidth-aware real-time exploration in mobile robot networks.  
1150 *Wireless Communications and Mobile Computing* 13, 9 (2013), 847–  
1151 863.
- 1152 [37] pytorch. 2024. pytroch. <https://pytorch.org/>.
- 1153 [38] Yi Ren, Chih-Wei Tung, Jyh-Cheng Chen, and Frank Y Li. 2018. Proportional  
1154 and preemption-enabled traffic offloading for IP flow mobility:  
1155 Algorithms and performance evaluation. *IEEE Transactions on Vehicular  
1156 Technology* 67, 12 (2018), 12095–12108.
- 1157 [39] Nurul I Sarkar and Osman Mussa. 2013. The effect of people movement  
1158 on Wi-Fi link throughput in indoor propagation environments. In *IEEE  
1159 2013 Tencon-Spring*. IEEE, 562–566.
- 1160 [40] Karen Simonyan and Andrew Zisserman. 2015. Very Deep  
1161 Convolutional Networks for Large-Scale Image Recognition.  
1162 arXiv:1409.1556 [cs.CV]
- 1163 [41] Debjyoti Sinha and Mohamed El-Sharkawy. 2019. Thin mobilenet: An  
1164 enhanced mobilenet architecture. In *2019 IEEE 10th annual ubiquitous  
1165 computing, electronics & mobile communication conference (UEMCON)*.  
1166 IEEE, 0280–0285.
- 1167 [42] Sasha Targ, Diogo Almeida, and Kevin Lyman. 2016. Resnet in resnet:  
1168 Generalizing residual architectures. *arXiv preprint arXiv:1603.08029*  
1169 (2016).
- 1170 [43] Hao Wang, Sreeram Potluri, Miao Luo, Ashish Kumar Singh, Sayantan  
1171 Sur, and Dhabaleswar K Panda. 2011. MVAPICH2-GPU: optimized  
1172 GPU to GPU communication for InfiniBand clusters. *Computer Science-  
1173 Research and Development* 26, 3 (2011), 257–266.
- 1174 [44] Junming Wang, Zekai Sun, Xiuxian Guan, Tianxiang Shen, Zongyuan  
1175 Zhang, Tianyang Duan, Dong Huang, Shixiong Zhao, and Heming Cui.  
1176 2024. AGRNav: Efficient and Energy-Saving Autonomous Navigation  
1177 for Air-Ground Robots in Occlusion-Prone Environments. In *IEEE  
1178 International Conference on Robotics and Automation (ICRA)*.
- 1179 [45] Lin Wang and Kuk-Jin Yoon. 2021. Knowledge distillation and student-  
1180 teacher learning for visual intelligence: A review and new outlooks.  
1181 *IEEE transactions on pattern analysis and machine intelligence* 44, 6  
1182 (2021), 3048–3068.
- 1183 [46] Sanghyun Woo, Shoubhik Debnath, Ronghang Hu, Xinlei Chen,  
1184 Zhuang Liu, In So Kweon, and Saining Xie. 2023. Convnext v2: Co-  
1185 designing and scaling convnets with masked autoencoders. In *Pro-  
1186 ceedings of the IEEE/CVF Conference on Computer Vision and Pattern  
1187 Recognition*. 16133–16142.
- 1188 [47] Huaming Wu, William J Knottenbelt, and Katinka Wolter. 2019. An  
1189 efficient application partitioning algorithm in mobile environments.  
1190 *IEEE Transactions on Parallel and Distributed Systems* 30, 7 (2019),  
1191 1464–1480.
- 1192 [48] Tianyu Wu, Shizhu He, Jingping Liu, Siqi Sun, Kang Liu, Qing-Long  
1193 Han, and Yang Tang. 2023. A brief overview of ChatGPT: The history,  
1194 status quo and potential future development. *IEEE/CAA Journal of  
1195 Automatica Sinica* 10, 5 (2023), 1122–1136.
- 1196 [49] Zhaoyang Xia, Youquan Liu, Xin Li, Xinge Zhu, Yuexin Ma, Yikang Li,  
1197 Yuenan Hou, and Yu Qiao. 2023. SCPNet: Semantic Scene Completion  
1198 on Point Cloud. In *Proceedings of the IEEE/CVF Conference on Computer  
1199 Vision and Pattern Recognition*. 17642–17651.
- 1200 [50] Yecheng Xiang and Hyoseung Kim. 2019. Pipelined data-parallel  
1201 CPU/GPU scheduling for multi-DNN real-time inference. In *2019 IEEE  
1202 Real-Time Systems Symposium (RTSS)*. IEEE, 392–405.
- 1203 [51] Jing Xu, Yu Pan, Xinglin Pan, Steven Hoi, Zhang Yi, and Zenglin Xu.  
1204 2022. RegNet: self-regulated network for image classification. *IEEE  
1205 Transactions on Neural Networks and Learning Systems* (2022).
- 1206 [52] Min Xue, Huaming Wu, Guang Peng, and Katinka Wolter. 2021.  
1207 DDPQN: An efficient DNN offloading strategy in local-edge-cloud  
1208 collaborative environments. *IEEE Transactions on Services Computing*  
1209 15, 2 (2021), 640–655.
- 1210 [53] Xinlei Yang, Hao Lin, Zhenhua Li, Feng Qian, Xingyao Li, Zhiming He,  
1211 Xudong Wu, Xianlong Wang, Yunhao Liu, Zhi Liao, et al. 2022. Mobile  
1212 access bandwidth in practice: Measurement, analysis, and implications.  
1213 In *Proceedings of the ACM SIGCOMM 2022 Conference*. 114–128.
- 1214 [54] Yang Yang, Li Juntao, and Peng Lingling. 2020. Multi-robot path  
1215 planning based on a deep reinforcement learning DQN algorithm.  
1216 *CAAI Transactions on Intelligence Technology* 5, 3 (2020), 177–183.
- 1217 [55] Yonghao Zhuang, Hexu Zhao, Lianmin Zheng, Zhuohan Li, Eric Xing,  
1218 Qirong Ho, Joseph Gonzalez, Ion Stoica, and Hao Zhang. 2023. On  
1219 optimizing the communication of model parallelism. *Proceedings of  
1220 Machine Learning and Systems* 5 (2023).